

Synthesis and Characterization of Porous Hydrogel Based on Lignin and Polyacrylamide

Qinghua Feng,^{a,b} Jinling Li,^a Heli Cheng,^a Fangeng Chen,^{c,*} and Yimin Xie^{a,*}

A porous lignin-containing hydrogel was developed for dye removal via graft copolymerization of acetic acid lignin (AAL) and acrylamide (AAm), in the presence of ethyleneglycol dimethacrylate (EGDMA) as a crosslinker and H₂O₂ as an initiator. AAL was characterized by FT-IR and TGA. After being washed to remove impurities, the hydrogel was characterized by FT-IR, TGA, SEM, and swelling ratio. FT-IR spectra suggested that AAL was present in the hydrogel. The TGA curves revealed that the introduction of AAL had no significant impact on the thermal stability of PAAm. SEM images showed that the honeycomb-like structure of the hydrogel was improved with increasing AAL content. The swelling ratio data showed that the hydrogel with a high AAL/AAm ratio was sensitive to pH. Furthermore, increased lignin content of the hydrogel favors the dye adsorption.

Keywords: Acetic acid lignin; Hydrogel; Polyacrylamide; Porous structure; Dye removal

Contact information: a: Hubei Provincial Key Laboratory of Green Materials for Light Industry, Hubei University of Technology, Wuhan 430068, China; b: Key Laboratory of Pulp and Paper Science & Technology of Ministry of Education, Qilu University of Technology, Jinan, 250353, China; c: State Key Laboratory of Pulp and Paper Engineering, South China University of Technology, Guangzhou 510640, China; *Corresponding author: fgchen@scut.edu.cn; ppymxie@scut.edu.cn

INTRODUCTION

Lignin, second only to cellulose in natural abundance, is an important constituent in biomass. The principal use for lignin is as a fuel to fire the boilers used for pulp production (Dimmel 2010). Moreover, lignin is now being isolated from the process of ethanol fuel production; commercial uses of the lignin by-product will greatly enhance the processing costs (Bujanovic *et al.* 2012). However, only 1 to 2% of lignin is isolated from pulping liquors and used to prepare polymer materials, *e.g.*, polyurethanes (Cinelli *et al.* 2013; Li and Ragauskas 2012; Pan and Saddler 2013), phenolic resins (Cheng *et al.* 2013), and epoxy resins (Qin *et al.* 2014; Sasaki *et al.* 2013). A review of materials prepared from lignin was presented by Chung and Washburn (2012).

In recent decades some lignin-based materials have been prepared from enzymatic hydrolysis lignin (Fang *et al.* 2010), acidic hydrolysis lignin (Da Silva *et al.* 2011), formic acid lignin (Consolin Filho *et al.* 2007), alkali lignin (Suteu *et al.* 2010), and lignosulfonate (Liu and Huang 2006) for removal of dyes from aqueous solution. The effectiveness of such systems has been attributed to various interactions, *e.g.*, electrostatic and hydrophobic interactions, between lignin and dyes (Hubbe *et al.* 2012). A hydrogel is a network of polymer chains that can absorb large amounts of water (Hennink and Van Nostrum 2012). Polyacrylamide (PAAm) hydrogels are also used extensively in dye wastewater treatment (Karadağ *et al.* 2002; Yang and Ni 2012) because of their three-dimensional cross-linked polymer networks of flexible chains that

are able to retain dye molecules. The porous structure networks allow dyes to diffuse through the hydrogel structure. As PAAm hydrogels possess anionic functional groups, they can absorb cationic dyes, *e.g.*, methylene blue (MB), from wastewaters (Yi and Zhang 2008). Due to the content of many anionic functional groups *e.g.*, phenolic and carboxylic groups, on the lignin, there is reason to expect cationic dye molecules to have good affinity with lignin-based PAAm hydrogel.

Acetic acid lignin (AAL) is a kind of organosolv lignin precipitated from the waste liquor of acetic acid pulping. Relatively little structural changes and condensed structure of AAL favor its reactivity (Feng and Chen 2012). In this study, AAL and MB was used as the lignin and cationic dye, respectively. A new kind of hydrogel derived from AAL and polyacrylamide was synthesized and characterized. The presence of AAL in the hydrogel was confirmed by FT-IR and TGA. The effect of lignin on the corresponding properties of the hydrogel was discussed.

EXPERIMENTAL

Materials

AAL was obtained from the acetic acid pulping of eucalyptus chips under atmospheric pressure (Uraki *et al.* 1991). AAL was deacetylated according to the method of our previous work (Feng *et al.* 2012). The \overline{M}_w and \overline{M}_n of AAL were 12060 and 5330 g/mol, respectively. The phenolic and carboxylic content of AAL was measured to be 2.42 and 0.09 mmol/g, respectively. Acrylamide (AAm, 99%) and ethyleneglycol dimethacrylate (EGDMA, 98%) were obtained from Aladdin Reagent Co. Ltd, Shanghai, China.

Methylene blue (MB) dye is a commercial product of Kermel Reagent Inc, China. The stock solution of 1.0 g/L MB was prepared by dissolving appropriate amount of MB in deionized water. The MB stock solution could be diluted to obtain solutions of different concentrations.

Methods

Preparation of the Hydrogels

The hydrogels were prepared according to the method of Meister and Chen (1991), with modifications. The compositions of these materials, based on the added amounts, are listed in Table 1.

Table 1. Feed Composition of the Hydrogels

Material \ Sample	PAAm	LGA1	LGA2	LGA3
AAL/g	0	0.5	0.5	0.5
AAm/g	3	2.5	3.5	4.5
EGDMA/ μ L	24	24	32	40
CaCl ₂ /g	0	0.3	0.4	0.5
30% H ₂ O ₂ / μ L	0	30	40	50
AIBN/g	0.03	0	0	0
DMSO/mL	3	3	4	5

Various amounts of CaCl₂ and 0.5 g of AAL were dissolved in DMSO successively. Then, the initiator, H₂O₂, was added to the solution. Subsequently, AAm and EGDMA were added to the solution. After being bubbled with N₂ for 20 min, the solution was placed in a 70 °C bath. The reaction was allowed to proceed for 12 h. Afterward, the gel was soaked in deionized water, where it was equilibrated for 7 days at ambient temperature. Deionized water was replaced every 12 h. Then, the hydrogel was carefully cut into small pieces for further characterization. In this paper, hydrogels prepared with 2.5, 3.5, and 4.5 g of AAm were named LGA1, LGA2, and LGA3, respectively.

PAAm hydrogel was synthesized for comparison. AAm and EGDMA were dissolved in DMSO successively. Then, 2,2-azobisisobutyronitrile (AIBN), the initiator, was added to the solution. After being bubbled with N₂ for 20 min, the solution was placed in a 70 °C bath for 12 h. The hydrogel was purified according to the method above.

Characterization of AAL, PAAm, and the Hydrogels

The FT-IR spectra of AAL, PAAm, and LGA2 were obtained on a Nicolet Nexus 670 Fourier transform infrared spectrometer using the KBr pellet technique. The samples were scanned 32 times in the range of 4000 to 500 cm⁻¹.

Thermogravimetric analysis (TGA) of AAL, PAAm, and LGA2 was performed on a TA Instruments Q500 using approximately 5 mg of sample under nitrogen at a heating rate of 20 °C min⁻¹ in the temperature range from room temperature to 700 °C. All samples were vacuum-dried at -50 °C for 24 h and then dried in a vacuum oven at 40 °C for 12 h prior to FT-IR, SEM, and TGA measurements.

The freeze-dried hydrogels were fractured carefully in liquid nitrogen. After being sputter-coated with gold, the hydrogels were characterized with scanning electron microscopy (SEM) on an FEI Quanta 200 apparatus with an accelerating voltage of 20 kV.

The equilibrium swelling ratio of the hydrogels was measured in the pH range of 1 to 9, with an interval of 2. After being immersed in deionized water for 24 h at each temperature, the hydrogel was taken out from water and blotted with wet filter paper to remove excess water on the hydrogel surface. The weight of wet hydrogel was recorded. The swelling ratio was calculated as follows,

$$\text{Swelling Ratio (\%)} = (W_s - W_d) / W_d \times 100 \quad (1)$$

where W_s and W_d represent the weight of swollen and dry hydrogel, respectively.

The swollen hydrogel sample was dried in a vacuum oven at 40 °C overnight until a constant weight was reached. The dried sample was immersed in deionized water at 25 °C and removed from water at pre-determined time intervals. Then, it was removed from water and blotted with wet filter paper to remove excess water on the hydrogel surface. The weight of wet hydrogel was recorded. The swelling ratio as a function of time was defined as follows,

$$\text{Swelling Ratio (\%)} = ((W_t - W_d) / W_d) \times 100 \quad (2)$$

where W_t is the weight of the wet hydrogel at time t and W_d is the same as defined above.

Equilibrium studies

The impact of initial dye concentration on the amount of MB removal was studied in a batch mode of operation for 72 h. In each adsorption experiment, 50 mL of MB solution with predetermined concentration and pH was stirred (100 rpm) with 0.1 g of the vacuum dried hydrogel at 30 °C, which was more than sufficient to reach equilibrium. The concentration in the supernatant solution was measured by monitoring the absorbance changes at a wavelength of maximum absorbance (664 nm) with a Beckman DU-7HS UV spectrophotometer. All the experiments were carried out at pH 5.0. The adsorption capacity of MB on the adsorbent was calculated by the following equation:

$$q_e = \frac{(C_0 - C_e)V}{m} \quad (3)$$

where q_e (mg/g) is the amount of MB adsorbed on the hydrogel, C_0 and C_e (mg/L) are the initial concentration and the equilibrium concentration of MB solution, respectively, V (L) represents the volume of solution treated, and m (g) represents the amount of the hydrogel added.

Kinetics studies

Vacuum dried LGA1 (2.0 g) was transferred into 1000 mL of MB solution (75 mg/L) at pH 5.0. The mixtures were stirred (100 rpm) at 30 °C. 2 mL MB solution were withdrawn at predetermined time intervals and measured as above. The amount of adsorption at time t , q_t (mg/g), was calculated as follows:

$$q_t = \frac{(C_0 - C_t)V}{m} \quad (4)$$

where C_t (mg/L) represents the concentration of MB solution at the predetermined time t and the other symbols are the same as defined above.

RESULTS AND DISCUSSION

Synthesis of the LGA Hydrogels

The mechanism of LGA hydrogel formation is shown in Fig. 1.

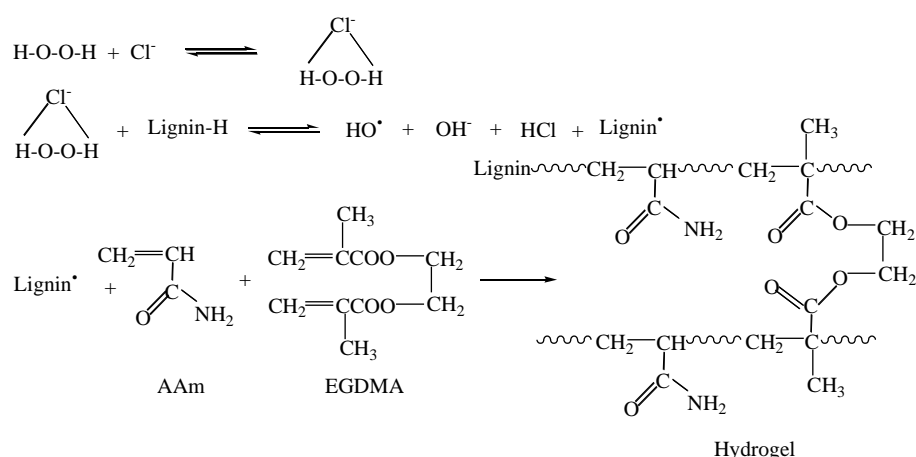


Fig. 1. Synthesis of the LGA hydrogels

During the formation of the hydrogels, hydroperoxide reacted with chloride anion to form a chlorine atom. Chlorine then abstracted hydrogen from lignin to form a free-radical site on the lignin. Subsequently, the lignin initiated polymerization. The LGA hydrogels can be easily synthesized in the presence of EGDMA.

FT-IR Spectra

The FT-IR spectra of AAL, LGA2, and PAAm are shown in Fig. 2. The spectrum of LGA2 shows a series of characteristic bands that can be assigned to the specific structures of AAL and PAAm that make up the hydrogel. The bands at 1660 and 1610 cm^{-1} are assigned to typical amide groups in PAAm and LGA2. A broad band at 3400 to 3200 cm^{-1} in the spectrum of LGA2 is attributed to the stretching of N–H (from PAAm). In comparison, the spectrum of LGA2 provides evidence of the existence of AAL in LGA hydrogels by showing the presence of the bands at 1505 and 1030 cm^{-1} . The band at 1505 cm^{-1} is characterized by the C=C stretching in aromatic rings. The absorption at 1030 cm^{-1} arises from C–O stretching in primary alcohol. The intensity of the band at 1130 cm^{-1} for C–O stretching in ether also increased.

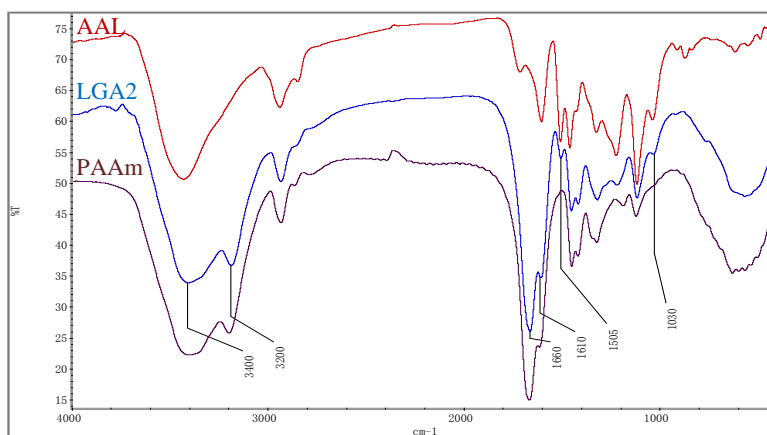


Fig. 2. FT-IR spectra of AAL, LGA2, and PAAm

Thermogravimetric Analysis

Figures 3 and 4 show the thermal stability, as evaluated by thermogravimetry, of AAL, PAAm, and LGA2. As shown, LGA2 and PAAm had similar TGA and DTG curves.

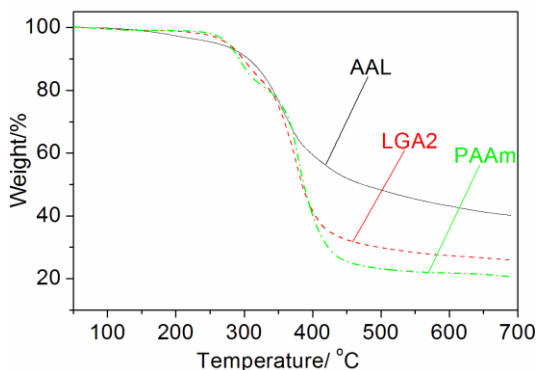


Fig. 3. TG curves of AAL, PAAm, and LGA2

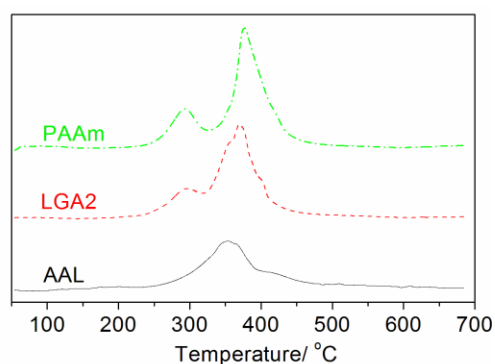


Fig. 4. DTG curves of AAL, PAAm, and LGA2

The temperature at 5% weight loss remained almost the same when AAL was incorporated into PAAM in the hydrogel. The results mean that the introduction of AAL had no negligible impact on the thermal stability of PAAM. Figure 3 also plots the impact of the introduction of AAL on the char residue percentage of LGA2. The fact that the char residue was higher in LGA2 than in PAAM confirmed the presence of AAL in LGA hydrogel. A similar trend in the TGA curves of lignin-g-Poly(N-isopropylacrylamide) hydrogels was observed in our previous work (Feng *et al.* 2011). However, the DTG curve of LGA2 in Fig. 4 showed four peaks, which is different from that of PAAM hydrogels (Caulfield *et al.* 2002). The results may be attributed to the high lignin content of LGA2 in the present work.

Interior Morphology

The interior morphology of the LGA hydrogels, obtained by freeze fracturing, is shown in Fig. 5. The images show that the honeycomb-like structure of the hydrogel was improved with increasing AAL content. The pore size of these porous structures changed little with increasing AAL/AAM ratio in the hydrogel composition. A contrasting result, however, was reported in our previous work (Feng *et al.* 2011), in which the pore size of lignin-g-poly(N-isopropylacrylamide) hydrogels increased with increasing lignin content. The result can be attributed to two possible explanations. First, the lignin content of the lignin-g-polyacrylamide hydrogels changed less than did that of lignin-g-poly(N-isopropylacrylamide) hydrogels. Second, polyacrylamide is more hydrophilic than poly(N-isopropylacrylamide).

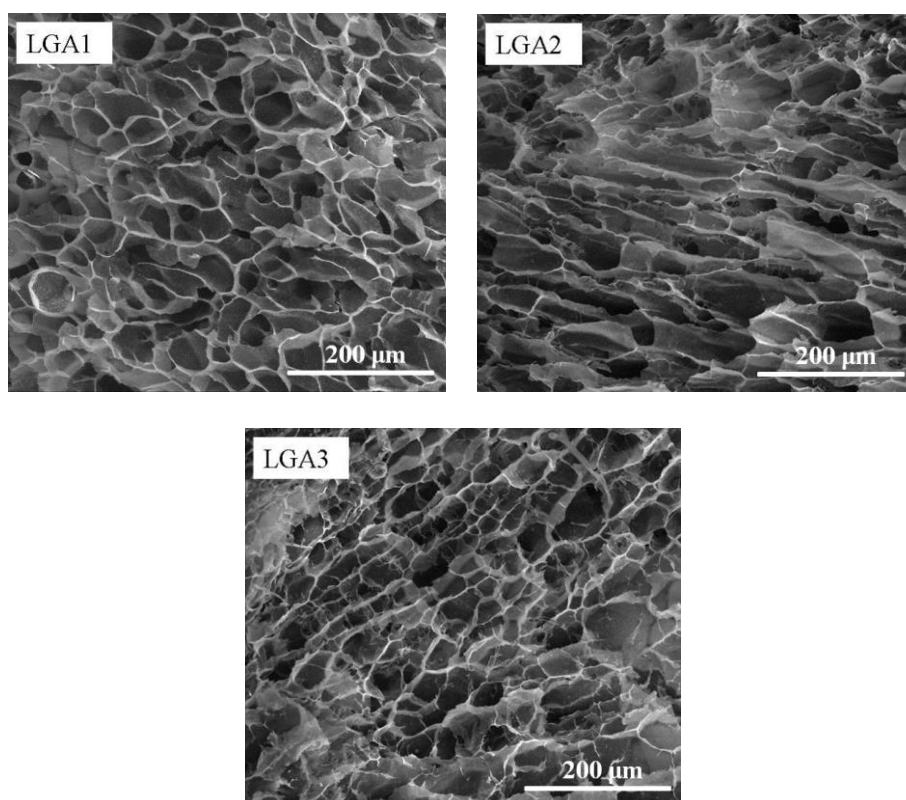


Fig. 5. SEM micrographs of the LGA hydrogels

The hydrophilic polyacrylamide highlighted the interaction of lignin in the hydrogel. Subsequently, physical crosslinking increased due to the interaction of lignin. The increased crosslinking decreased the pore size of the high-lignin content polyacrylamide hydrogel.

Swelling Ratio

Figure 6 shows the swelling ratios of the hydrogels as a function of time in deionized water. The curves indicate that the swelling ratios of the hydrogels increased as the content of the hydrophobic component (AAL) decreased. This means that water diffused into the LGA hydrogels network more slowly with higher AAL content. Specifically, LGA3 exhibited a relatively fast swelling rate, reaching a swelling ratio of around 930% within 420 min, while the swelling ratio of LGA1 was less than 750%. This tendency may be attributed to the incorporation of hydrophobic AAL (Lee and Yeh 2005).

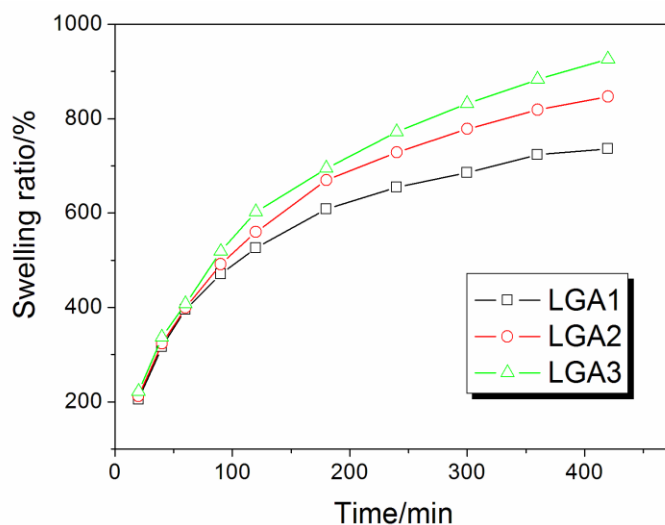


Fig. 6. Swelling ratios of the LGA hydrogels as a function of time

Figure 7 shows the swelling ratios as functions of pH for the LGA hydrogels.

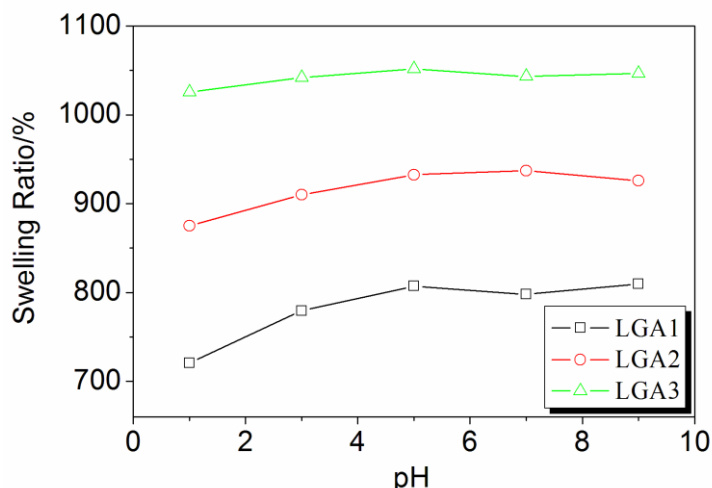


Fig. 7. Effect of pH on the swelling ratios of the LGA hydrogels

The effect of pH was most pronounced in LGA1, and the swelling ratio increased with increasing medium pH. This could be attributed to the relatively low AAL content of LGA2 and LGA3. Decreasing pH will tend to make the network more condensed because of carboxylic groups on the AAL, since those groups are protonated and uncharged at low pH. Furthermore, the LGA hydrogels were only slightly sensitive to pH due to the low amount of carboxylic acid groups in AAL (Zhang *et al.* 2004).

Adsorption Isotherms

Langmuir and Freundlich isotherms are often used to describe and understand the mechanism of the adsorption. The Langmuir model is based on monolayer adsorption (Langmuir 1918), while the Freundlich isotherm model assumes heterogeneity of adsorption surfaces (Freundlich 1906). The equation can be expressed in the following equations:

$$\frac{C_e}{q_e} = \frac{1}{q_0 K_L} + \frac{C_e}{q_0} \quad (5)$$

$$\log q_e = \log K_F + \frac{1}{n} \log C_e \quad (6)$$

where q_0 (mg g^{-1}) and K_L (L mg^{-1}) represent the monolayer adsorption capacity and Langmuir constant, respectively. Values of q_0 and K_L were calculated from the plot of C_e/q_e against C_e . K_F ($\text{mg}^{1-1/n} \text{L}^{1/n} \text{g}^{-1}$) and n represent the constants related to sorption capacity and sorption intensity of adsorbents, respectively. The values of K_F and n were determined from the slopes and intercepts of the plots of $\log q_e$ versus $\log C_e$; their values are given in Table 2.

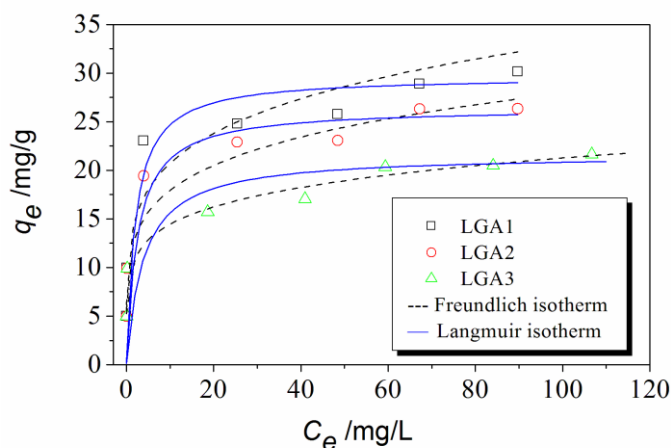


Fig. 8. Equilibrium curves (V , 25 mL; m , 0.25 g; pH, 5.0; temperature, 30 °C)

The isotherm constants can be utilized to predict whether an adsorption system is favorable or unfavorable. The essential characteristics of the Langmuir isotherm can be expressed in terms of a dimensionless constant separation factor or an equilibrium parameter, R_L , which is expressed by:

$$R_L = \frac{1}{1 + K_L C_0} \quad (7)$$

where C_0 (mg L^{-1}) represents the highest initial dye concentration. As shown in Table 2, the R_L values of LGA hydrogels were found to be between 0 and 1, indicating that LGA hydrogel favors the adsorption of MB. The n values in the Freundlich equation can also indicate how favorable an adsorbent is to adsorb the adsorbate. The result showed that the values of n were all in the range of 1 to 10, which implies that dye molecules are favorably adsorbed by the LGA hydrogel. This is in good agreement with other findings regarding the R_L value (Chen *et al.* 2011).

Table 2. Isotherm Parameters (V , 50 mL; m , 0.1 g; pH, 5.0; temperature, 30 °C)

Isotherm model		LGA1	LGA2	LGA3
Langmuir	q_0 (mg g^{-1})	29.65	26.43	21.62
	K_L (L mg^{-1})	0.4963	0.4004	0.2597
	R_L	0.01325	0.01638	0.02503
	r_L^2	0.9928	0.9937	0.9900
Freundlich	K_F ($\text{mg}^{1-1/n} \text{L}^{1/n} \text{g}^{-1}$)	13.0529	11.5361	9.8117
	n	4.9857	5.2134	5.9557
	r_F^2	0.9396	0.9696	0.9191

The coefficients of determination (r_L^2 and r_F^2), as listed in Table 2, indicated that the experimental equilibrium data matched the Langmuir model better than the Freundlich model. This suggested the monolayer coverage of MB onto the LGA hydrogel. The adsorption capacity of LGA hydrogel was increased with increasing AAL content due to anionic functional groups of lignin.

Adsorption Kinetics

Figure 9 shows the adsorption capacity of the adsorbent as a function of time under the condition of a dye initial concentration of 75 mg/L.

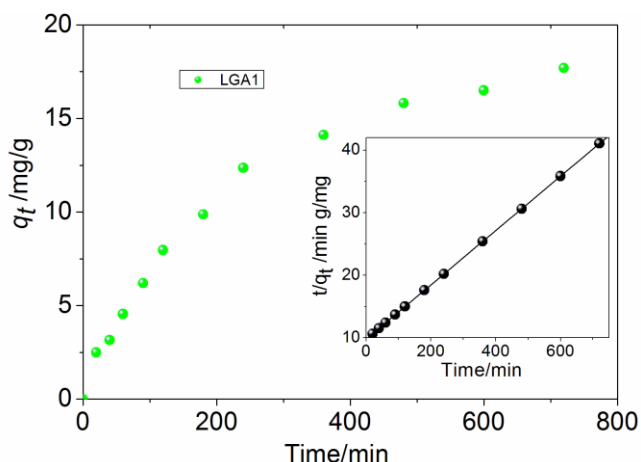


Fig. 9. Adsorption kinetics curve and pseudo-second order plot for the adsorption of MB on LGA1

As can be seen in the figure, the dye adsorption process on the LGA1 was rapid in the first 20 min, and thereafter it proceeded at a slower rate, then rapid again during the 40-60 min. The relatively high adsorption rate in the initial 20 min may be due to the highest levels of vacant site on hydrogel surface. Dry hydrogel sample prevented dyes diffusion during the 20 to 40 min. As hydrogel adsorbed water, its structure became porous, leading to dyes diffusion through the hydrogel structure. Therefore, the adsorption rate was high again.

In order to investigate dye adsorption rate, the kinetics of MB adsorption by LGA1 was modelled using pseudo-first order and pseudo-second order shown below as equations (8) and (9), respectively:

$$\frac{1}{q_t} = \frac{k_1}{q_e t} + \frac{1}{q_e} \quad (8)$$

$$\frac{t}{q_t} = \frac{1}{k_2 q_e^2} + \frac{t}{q_e} \quad (9)$$

where k_1 (min^{-1}) and k_2 ($\text{g mg}^{-1} \text{min}^{-1}$) are the rate constants of pseudo-first-order and pseudo-second-order, respectively.

The models parameters and regression coefficients (r^2) were determined by linear regression analysis and are listed in Table 3. According to the linear pseudo-second order plot obtained by plotting t/q_t against t (inset in Fig. 9) and the r^2 value, it clearly shows that MB adsorption data on the hydrogel were successfully described by pseudo-second order model. Similar phenomena have been observed in the adsorption of anionic dyes on other hydrogel with anionic functional groups modified by PAAm (Yang *et al.* 2013).

Table 3. Pseudo-first order and pseudo-second order kinetic parameters for MB adsorption on LGA1 (C_0 : 75 mg/L).

$q_{e, exp}$ (mg g^{-1})	Pseudo-first-order			Pseudo-second-order		
	k_1 (min^{-1})	$q_{e, cal}$ (mg g^{-1})	r_1^2	k_2 (min^{-1})	$q_{e, cal}$ (mg g^{-1})	r_2^2
24.79	124.93	16.34	0.9392	0.0001927	23.03	0.9900

CONCLUSIONS

1. pH-sensitive hydrogels containing AAL and PAAm were prepared *via* graft polymerization in the presence of EGDMA as the crosslinker and H_2O_2 as the initiator.
2. The thermal stability of the hydrogels was not influenced by the introduction of AAL. The interior network of the hydrogels was porous, and the pore size remained almost the same when the weight ratio of AAL/AAM increased from 1/5 to 1/9. The swelling ratio decreased with increasing AAL/AAM ratio.
3. The adsorption of methylene blue (MB) for hydrogels were found to be highly dependent on lignin content. High lignin content favors the adsorption of MB. The maximum adsorption capacity was 29.65 mg MB per gram of LGA hydrogel.

ACKNOWLEDGMENTS

The authors are grateful for the kind support from the Committee of the 4th Conference on Biorefinery towards Bioenergy (ICBB2013) in Xiamen, China. This work was financially supported by Scientific Research Fund of Hubei Provincial Department of Education (Q20141402), the Foundation (08031348) of Key Laboratory of Pulp and Paper Science & Technology of Ministry of Education, Qilu University of Technology, China, and the Priming Scientific Research Foundation for Ph.D. teachers at HBUT (BSQD12136).

REFERENCES CITED

- Bujanovic, B. M., Goundalkar, M. J., and Amidon, T. E. (2012). "Increasing the value of a biorefinery based on hot-water extraction: Lignin products," *Tappi J.* 11(1), 19-26.
- Caulfield, M. J., Qiao, G. G., and Solomon, D. H. (2002). "Some aspects of the properties and degradation of polyacrylamides," *Chem. Rev.* 102(9), 3067-3084.
- Chen, H., Zhao, J., Wu, J. Y., and Dai, G. L. (2011). "Isotherm, thermodynamic, kinetics and adsorption mechanism studies of methyl orange by surfactant modified silkworm exuviae," *J. Hazard. Mater.* 192(1), 246-254.
- Cheng, S. N., Yuan, Z. S., Leitch, M., Anderson, M., and Xu, C. C. (2013). "Highly efficient de-polymerization of organosolv lignin using a catalytic hydrothermal process and production of phenolic resins/adhesives with the depolymerized lignin as a substitute for phenol at a high substitution ratio," *Ind. Crops Prod.* 44, 315-322.
- Chung, H., and Washburn, N. R. (2012). "Chemistry of lignin-based materials," *Green Mater.* 1(3), 137-160.
- Cinelli, P., Anguillesi, I., and Lazzeri, A. (2013). "Green synthesis of flexible polyurethane foams from liquefied lignin," *Eur. Polym. J.* 49(6), 1174-1184.
- Consolin Filho, N., Venancio, E.C., Barriquello, M.F., Hechenleitner, A.A.W., and Pineda, E.A.G. (2007). "Methylene blue adsorption onto modified lignin from sugar cane bagasse," *Ecl. Quím (São Paulo)* 32(4), 63-70.
- Da Silva, L. G., Ruggiero, R., Gontijo, P. D. M., Pinto, R. B., Royer, B., Lima, E. C., Fernandes, T. H. M., and Calvete, T. (2011). "Adsorption of Brilliant Red 2BE dye from water solutions by a chemically modified sugarcane bagasse lignin," *Chem. Eng. J.* 168(2), 620-628.
- Dimmel, D. (2010). "Overview," in: *Lignin and Lignans: Advances in Chemistry*, C. Heitner, D. Dimmel, and J. Schmidt (eds.), CRC Press, Boca Raton.
- Fang, R., Cheng, X.S., and Xu, X.R. (2010). "Synthesis of lignin-base cationic flocculant and its application in removing anionic azo-dyes from simulated wastewater," *Bioresour. Technol.* 101(19), 7323-7329.
- Feng, P., and Chen, F. G. (2012). "Preparation and characterization of acetic acid lignin-based epoxy blends," *BioResources* 7(3), 2860-2870.
- Feng, Q. H., Chen, F. G., and Wu, H. R. (2011). "Preparation and characterization of a temperature-sensitive lignin-based hydrogel," *BioResources* 6(4), 4942-4952.

- Feng, Q. H., Chen, F. G., and Zhou, X. S. (2012). "Preparation of thermo-sensitive hydrogels from acrylated lignin and N-isopropylacrylamide through photocrosslinking," *J. Biobased Mat. Bioen.* 6(3), 336-342.
- Freundlich, H. M. F. (1906). "Over the adsorption in solution," *J. Phys. Chem.* 57, 385-470.
- Hennink, W. E., and Van Nostrum, C. F. (2012). "Novel crosslinking methods to design hydrogels," *Adv. Drug Delivery Rev.* 64(Supplement), 223-236.
- Hubbe, M. A., Beck, K. R., O'Neal, W. G., and Sharma, Y. C. (2012). "Cellulosic substrates for removal of pollutants from aqueous systems: A review. 2. Dyes," *BioResources* 7(2), 2592-2687.
- Karadağ, E., Üzümlü, Ö. B., and Saraydın, D. (2002). "Swelling equilibria and dye adsorption studies of chemically crosslinked superabsorbent acrylamide/maleic acid hydrogels," *Eur. Polym. J.* 38(11), 2133-2141.
- Langmuir, I. (1918). "The adsorption of gases on plane surfaces of glass, mica and platinum," *J. Am. Chem. Soc.* 40(9), 1361-1403.
- Lee, W. F., and Yeh, Y. C. (2005). "Studies on preparation and properties of NIPAAm/hydrophobic monomer copolymeric hydrogels," *Eur. Polym. J.* 41(10), 2488-2495.
- Li, Y., and Ragauskas, A. J. (2012). "Kraft lignin-based rigid polyurethane foam," *J. Wood Chem. Technol.* 32(3), 210-224.
- Liu, M. H., and Huang, J. H. (2006). "Removal and recovery of cationic dyes from aqueous solutions using spherical sulfonic lignin adsorbent," *J Appl. Polym. Sci.* 101(4), 2284-2291.
- Meister, J. J., and Chen, M. J. (1991). "Graft 1-phenylethylene copolymers of lignin. 1. Synthesis and proof of copolymerization," *Macromolecules* 24(26), 6843-6848.
- Pan, X. J., and Saddler, J. N. (2013). "Effect of replacing polyol by organosolv and kraft lignin on the property and structure of rigid polyurethane foam," *Biotechnol. Biofuel.* 6(1), 12-21.
- Qin, J. L., Wolcott, M., and Zhang, J. W. (2014). "Use of polycarboxylic acid derived from partially depolymerized lignin as a curing agent for epoxy application," *ACS Sustainable Chem. Eng.* 2 (2), 188-193.
- Sasaki, C., Wanaka, M., Takagi, H., Tamura, S., Asada, C., and Nakamura, Y. (2013). "Evaluation of epoxy resins synthesized from steam-exploded bamboo lignin," *Ind. Crops Prod.* 43, 757-761.
- Suteu, D., Malutan, T., and Bilba, D. (2010). "Removal of reactive dye Brilliant Red HE-3B from aqueous solutions by industrial lignin: Equilibrium and kinetics modeling," *Desalination* 255(1), 84-90.
- Uraki, Y., Sano, Y., and Sasaya, T. (1991). "Cooking of hardwoods with organosolv pulping in aqueous acetic acid containing sulfuric acid at atmospheric pressure," *Jpn. TAPPI J.* 45(9), 1018-1024.
- Yang, X. J., and Ni, L. (2012). "Synthesis of hybrid hydrogel of poly (AM co DADMAC)/silica sol and removal of methyl orange from aqueous solutions," *Chem. Eng. J.* 209, 194-200.

- Yang, Y. F., Xie, Y. L., Pang, L. C., Li, M., Song, X. H., Wen, J. G., and Zhao, H. Y. (2013). "Preparation of reduced graphene oxide/poly (acrylamide) nanocomposite and its adsorption of Pb (II) and methylene blue," *Langmuir* 29(34), 10727-10736.
- Yi, J. Z., and Zhang, L. M. (2008). "Removal of methylene blue dye from aqueous solution by adsorption onto sodium humate/polyacrylamide/clay hybrid hydrogels," *Bioresour. Technol.* 99(7), 2182-2186.
- Zhang, X. Z., Wu, D. Q., and Chu, C. C. (2004). "Synthesis and characterization of partially biodegradable, temperature and pH sensitive Dex-MA/PNIPAAm hydrogels," *Biomaterials* 25(19), 4719-4730.

Article submitted: January 21, 2014; Peer review completed: March 29, 2014; Revised version received: May 23, 2014; Accepted: June 1, 2014; Published: June 4, 2014.